Synchronization in interacting populations of heterogeneous oscillators with time-varying coupling

Paul So,[a)] Bernard C. Cotton,[b)] and Ernest Barreto[c)]
*Department of Physics & Astronomy, The Center for Neural Dynamics, and The Krasnow Institute
for Advanced Study, George Mason University, Fairfax, Virginia 22030, USA*

In many networks of interest (including technological, biological, and social networks), the connectivity between the interacting elements is not static, but changes in time. Furthermore, the elements themselves are often not identical, but rather display a variety of behaviors, and may come in different classes. Here, we investigate the dynamics of such systems. Specifically, we study a network of two large interacting heterogeneous populations of limit-cycle oscillators whose connectivity switches between two fixed arrangements at a particular frequency. We show that for sufficiently high switching frequency, this system behaves as if the connectivity were static and equal to the time average of the switching connectivity. We also examine the mechanisms by which this fast-switching limit is approached in several nonintuitive cases. The results illuminate novel mechanisms by which synchronization can arise or be thwarted in large populations of coupled oscillators with nonstatic coupling. © *2008 American Institute of Physics*.
[DOI: 10.1063/1.2979693]

Recently, a great deal of attention has been paid to networks of interacting components in physical, biological, technological, social, and other contexts.[1] Most of this work assumes that the connectivity of the network of interest is static. However, in real networks of such units (i.e., physical, biological, social, etc.), communication among the individual components is often not independent of time. The coupling strength, the type of coupling, and the connection topology may not necessarily remain constant, and the rate of change of connectivity may range from slow to fast. Here, we use a recently published model system[8] consisting of a network of two interacting populations of oscillators to examine the dynamical consequences of time-varying connectivity. Specifically, our system consists of two interacting populations of globally coupled heterogeneous limit-cycle oscillators (Kuramoto systems) in which the relative strengths of the intra- and interpopulation couplings are specified by a two-by-two matrix. Knowledge of this matrix is sufficient to determine whether or not the system will exhibit collective synchronous behavior. We introduce time-dependent connectivity by alternately switching the coupling matrix between two specified matrices at a fixed frequency. We show that as the frequency of switching increases, the network's behavior approaches that of a nonswitching network described by the time-averaged connectivity. In addition, we examine the mechanisms by which this fast-switching limit is approached in several nonintuitive cases. Our results extend previous results reported in the literature[3–5] to both systems of heterogeneous elements and to systems consisting of multiple subpopulations. Importantly, our results illuminate novel mechanisms by which synchronization may arise or be thwarted as a result of interpopulation dynamics, and we explain these mechanisms in terms of the interactions between the order parameter phasors corresponding to each population. We believe that these mechanisms are broadly relevant in light of recent results[8,14] indicating that many networks of interest consist of interacting clusters or communities of elements.

I. INTRODUCTION

An early example of work considering time-dependent coupling cited possible applications in communication and in spike-coupled networks.[2] These authors considered the asymptotic stability of a unidirectionally coupled pair of identical systems in which the state variables involved in the coupling were periodically reset to new values. It was proven that if the frequency of this driving is high enough and the continuously driven system is asymptotically stable, then the periodically driven system is also asymptotically stable.

In more recent work, the authors of Refs. 3 studied synchronization in a population of chaotic dynamical systems with time-dependent connectivity using a master stability function framework. The stated motivation of these authors was, in part, the study of disease propagation in social networks and the coordinated control of platoons of autonomous vehicles. A similar approach was used in Ref. 4. Meanwhile, the authors of Ref. 5, citing both neurobiological and technological motivations (such as the synchronization of clocks over the internet), considered synchronization in time-dependent small-world networks using a Lyapunov function approach. In their formulation, random small-world connections were added to a pristine nearest-neighbor network of

a)Electronic mail: paso@gmu.edu. Web page: http://complex.gmu.edu/~paso.
b)Electronic mail: bcotton@gmu.edu.
c)Electronic mail: ebarreto@gmu.edu. Web page: http://complex.gmu.edu/~ernie.

18, 037114-1

dynamical systems as in the usual case, but the small-world connections were removed and reassigned periodically in time. In all these references, the authors showed that if the connection switching in their respective systems occurs quickly enough, their systems behave as if the coupling were static and equal to the time average of the switching connectivity.

The stability analysis that leads to these results relies on the assumption that the network consists of a single population of identical elements. In this paper, we consider synchronization in time-dependent networks of more than one population of heterogeneous elements. We draw motivation from the observation that the individual elements of a neurobiological network are never homogeneous. In fact, there is a great variety of different classes of neurons, each of which has its own diverse repertoire of behavior. The same can be said of proteins in metabolic networks, individuals in social networks, etc.

The paradigm for the study of synchronization in a heterogeneous network of oscillators is the Kuramoto system.[6] This consists of a large (or infinite) population of limit cycle oscillators in which the natural unperturbed frequency for each oscillator is drawn at random from a given distribution function. When uncoupled, these oscillators behave incoherently. But with sufficiently strong coupling, coherent collective behavior spontaneously emerges—that is, the oscillators synchronize. Kuramoto assumed a particular form for the oscillator interaction and was able to analytically determine the critical value of coupling for the onset of synchronization. This model, though rather abstract, has been enormously influential and has found many applications.[7]

In this paper, we consider the synchronization properties of multipopulation networks that are heterogeneous and have time-dependent coupling. We show that the fast-switching results described above are also valid in a more general heterogeneous context. The analysis presented here builds on, and is made possible by, previous results in which criteria for the onset of synchronization in a network-of-networks reformulation of the Kuramoto system with static connectivity were derived.[8]

The paper is organized as follows. In Sec. II, we briefly review the relevant previous results of Ref. 8, as well as general results for homogeneous switching systems. We introduce our heterogeneous switching system in Sec. III, and differentiate between the slow and fast switching limits. Various cases of interest are then considered in more detail. We conclude in Sec. IV.

II. REVIEW OF PREVIOUS RESULTS

A. Synchronization criteria in static networks

In previous work,[8] we obtained criteria for the occurrence of synchronization in a network of many interacting populations of limit-cycle oscillators with static coupling. We begin by reviewing the results of this work that are relevant to the current paper. Consider the following system of two interacting oscillator populations labeled θ and ϕ,

$$\frac{d\theta_i}{dt} = \omega_{\theta i} + \eta \frac{K_{\theta\theta}}{N_\theta} \sum_{j=1}^{N_\theta} \sin(\theta_j - \theta_i) + \eta \frac{K_{\theta\phi}}{N_\phi} \sum_{j=1}^{N_\phi} \sin(\phi_j - \theta_i),$$

$$i \in [1, N_\theta],$$

$$\frac{d\phi_i}{dt} = \omega_{\phi i} + \eta \frac{K_{\phi\theta}}{N_\theta} \sum_{j=1}^{N_\theta} \sin(\theta_j - \phi_i) + \eta \frac{K_{\phi\phi}}{N_\phi} \sum_{j=1}^{N_\phi} \sin(\phi_j - \phi_i),$$

$$i \in [1, N_\phi].$$

(1)

Here θ_i and ϕ_i are the phases of the individual oscillators in population θ and ϕ, respectively. We assume that the number of oscillators in each population (N_σ for $\sigma = \theta, \phi$) is very large, and that the natural frequencies $\omega_{\theta i}$ and $\omega_{\phi i}$ are drawn at random from two (possibly different) distributions $G_\sigma(\omega_\sigma)$. η is an overall coupling strength, and the connection matrix

$$\mathbf{K} = \begin{pmatrix} K_{\theta\theta} & K_{\theta\phi} \\ K_{\phi\theta} & K_{\phi\phi} \end{pmatrix}$$

characterizes the relative strengths of the intra- and interpopulation interactions. Here, we allow the individual elements $K_{\sigma\sigma'}$ within the connection matrix to be any real number. [Allowing these to be complex is equivalent to introducing phase shifts in the sine functions of Eq. (1).[8]]

Kuramoto defined a complex order parameter z which characterizes the degree of synchronization in the oscillator population. For our system, we use a separate order parameter for each population, i.e.,

$$z_\sigma \equiv r_\sigma e^{i\psi_\sigma} = \frac{1}{N_\sigma} \sum_{j=1}^{N_\sigma} e^{i\sigma_j}, \quad \sigma = \theta, \phi.$$

(2)

Intuitively, $r_\sigma = |z_\sigma|$ is the magnitude of the vector average of all the phasors that characterize the state of each individual oscillator in population σ. If the oscillators are incoherent, the phasors are uniformly distributed about the circle, and $r_\sigma = 0$. $r_\sigma = 1$ indicates that the oscillators are perfectly synchronized, and values of r_σ such that $0 < r_\sigma < 1$ correspond to states of partial synchronization. (In this work, the term "synchronization" refers to any state for which $r_\sigma > 0$.)

In the original Kuramoto system (i.e., only one population), the incoherent state ($r = 0$) is observed for zero coupling. As the coupling strength is increased, coherent collective behavior is not observed until a critical value of the coupling strength is reached. Beyond this value, r increases, indicating that the system spontaneously synchronizes.

Similar behavior is observed in our system of two interacting populations, but certain details depend on the connectivity matrix.[8] To obtain the criteria for synchronization, one can perform a linear stability analysis of the incoherent state, for which the order parameters r_σ are zero. One considers a small perturbation to this state and assumes that the perturbation evolves exponentially in time; thus the order parameters are written $\delta r_\sigma e^{st}$. If s has a negative real part, then this perturbation decays exponentially, and the incoherent state is stable. If s has a positive real part, then the perturbation grows exponentially, and the incoherent state is unstable. In this case, the system then evolves to a state that exhibits

synchronization with $r_\sigma \neq 0$. The critical state for the onset of synchronization, therefore, occurs for $\text{Re}(s)=0$.

For the system in Eq. (1), a self-consistency argument leads to the following equation for the order parameter perturbations:

$$\left[\eta \mathbf{K} - \begin{pmatrix} 1g_\theta(s) & 0 \\ 0 & 1g_\phi(s) \end{pmatrix} \right] \begin{pmatrix} \delta r_\theta e^{st} \\ \delta r_\phi e^{st} \end{pmatrix} = 0, \qquad (3)$$

where the complex function $g_\sigma(s)$ is defined by

$$g_\sigma(s) \equiv \frac{1}{2} \int_{-\infty}^{\infty} \frac{G_\sigma(\omega_\sigma)}{s - i\omega_\sigma} d\omega_\sigma.$$

Equation (3) has a nontrivial solution if the determinant of the matrix in the square brackets is zero. Given the natural frequency distributions $G_\sigma(\omega_\sigma)$ and the connectivity matrix $\mathbf{K}$, we set $\text{Re}(s)=0$, and the determinant condition determines the critical value(s) of the overall coupling strength η^* for the onset of synchronization.

For the special case in which $G_\sigma(\omega_\sigma)$ are Cauchy–Lorentz distributions with mean frequency Ω_σ and half-width at half-maximum Δ_σ, $G_\sigma(\omega_\sigma) = \Delta_\sigma / \{\pi \times [(\omega_\sigma - \Omega_\sigma)^2 + \Delta_\sigma^2]\}$, the zero determinant condition reduces to

$$[\eta K_{\theta\theta} - 2(iv + \Delta_\theta - i\Omega_\theta)][\eta K_{\phi\phi} - 2(iv + \Delta_\phi - i\Omega_\phi)] - \eta^2 K_{\theta\phi} K_{\phi\theta} = 0, \qquad (4)$$

where we have set $s=iv$ with v real. Equation (4) can be separated into its real and imaginary parts, resulting in two equations that can be solved simultaneously for the two unknowns η^* and v^*. In general, this may require numerical methods.[8]

Recently, Ott and Antonsen[20] introduced a novel method that allows one to reduce the problem in Eq. (1) (in the thermodynamic limit) into two coupled ODEs for the two complex order parameters. Following Kuramoto's original analysis, Ott and Antonsen started with the assumption that in the limit $N_\sigma \to \infty$, the oscillator network can be described by a continuous distribution function $f_\sigma(\omega_\sigma, \sigma, t)$ with $\int_0^{2\pi} f_\sigma(\omega_\sigma, \sigma, t) d\sigma = g_\sigma(\omega_\sigma)$. The key in this analysis was the introduction of a Fourier ansatz for the expansion of f_σ, i.e.,

$$f_\sigma = \frac{g_\sigma(\omega_\sigma)}{2\pi} \left\{ 1 + \left[\sum_{n=1}^{\infty} \alpha_\sigma^n(\omega_\sigma, t) e^{in\sigma} + \text{c.c.} \right] \right\},$$

where $|\alpha_\sigma(\omega_\sigma, t)| < 1$ to ensure the convergence of the series. With a few additional technical assumptions on $\alpha_\sigma(\omega_\sigma, t)$, the authors in Ref. 20 derived the following system of equations for a multipopulation network of phase oscillators with a Lorentzian frequency distribution:

$$\frac{dz_\sigma}{dt} = (i\Omega_\sigma - \Delta_\sigma)z_\sigma + \frac{\eta}{2} \sum_{\sigma'=\theta,\phi} K_{\sigma,\sigma'}[z_{\sigma'} - z_{\sigma'}^* z_\sigma^2], \qquad (5)$$

where $\sigma = \theta, \phi$. Equations (4) and (5) provide two alternative ways to analyze the coherence of two interacting populations of phase oscillators with static coupling.

In this paper, we set $\Omega_\theta = \Omega_\phi = \Omega$ and $\Delta_\theta = \Delta_\phi = \Delta$, i.e., the oscillator frequencies for each population are drawn from identical distributions. Ω can be set to zero without loss of

TABLE I. Formulas for η^*.

Condition	η^*
$T^2 > 4D$	$\Delta \left(\dfrac{T \pm \sqrt{T^2 - 4D}}{D} \right)$
$T^2 \leqslant 4D$	$\dfrac{4\Delta}{T}$
$D = 0$	$\dfrac{2\Delta}{T}$
$T = 0, D < 0$	$\pm \dfrac{2\Delta}{\sqrt{-D}}$
$T = 0, D \geqslant 0$	no solution

generality, and we also assume that the intrinsic properties of the oscillators do not change in time. In this case, an explicit solution to Eq. (4) can be easily expressed in terms of the trace T and determinant D of the connection matrix $\mathbf{K}$, and Δ. The solutions appear in Table I. Thus, we have a complete understanding of the criteria for synchronization in the system of Eq. (1). Given any connection matrix $\mathbf{K}$, overall coupling strength η, and the oscillator frequency distributions $G_\sigma(\omega_\sigma)$, we can determine if the system will synchronize or not. We conclude this section by drawing attention to one particular result that we will use later. If one adopts the assumptions described above (i.e., identical Cauchy–Lorentz frequency distributions), it can be shown (see Table I) that synchronization does not occur for any value of η if the connection matrix is traceless ($\text{tr}(\mathbf{K})=0$) and has a determinant greater than or equal to zero ($\det(\mathbf{K}) \geqslant 0$).

B. Switching networks

In the above discussion, the connection matrix and the coupling strength for the network are assumed to be static. For this study, we are interested in relaxing this assumption. For example, one can define a time-dependent system $\dot{x}(t) = f_{\rho(t)}(x(t))$ in terms of a switching sequence $\rho(t) : \mathbb{R} \to \mathbb{S} \subset \mathbb{Z}_+$. Here, $x(t)$ is the n-dimensional state vector. At each instant of time, its time evolution is determined by $f_{\rho(t)}$, in which $\rho(t)$ selects a particular function f_i from a collection $\{f_1, f_2, \cdots\}$.

In the simple situation in which this collection consists of linear systems such that the individual f_i are constant matrices $\mathbf{A}_i$, there is a wealth of established results concerning the stability of the switched system's equilibrium state.[9–13] In the most straightforward scenario, if the individual matrices $\mathbf{A}_i$ are all stable (i.e., all of their eigenvalues are negative), it can be shown that the switched system is stable if the switching is relatively slow. Intuitively, if the dwell time for each $\mathbf{A}_i$ is longer than the largest characteristic decay time of all the $\mathbf{A}_i$'s, then the system will spend most of the time very close to the corresponding stable equilibrium states. If the switching sequence is faster, one can often find a common Lyapunov function for all the $\mathbf{A}_i$, and therefore prove that the switched system is again stable.[9] In this situation, one can envision the trajectory of the switched system hopping

within a piecewise linear "potential well" such that the constituent pieces form a bowl shape with a local minimum at the equilibrium location.

Going one step further, consider the more natural case in which some or all of the $\mathbf{A}_i$'s within the switching set are not stable. It is still possible to have stability in the switched system if the switching sequence is chosen appropriately. In particular, an interesting fast-switching result exists. For some classes of linear systems with the following time parametrization: $\dot{x}(t) = \mathbf{A}_{\rho(t/\epsilon)} x(t)$, where $\epsilon > 0$, the switched system can be shown to be asymptotically stable for sufficiently small ϵ if the time-average system given by $\dot{x}(t) = \langle \mathbf{A} \rangle x(t)$, where $\langle \mathbf{A} \rangle = \lim_{T \to \infty} 1/T \int_0^T \mathbf{A}_{\rho(t)} dt$, is also asymptotically stable.[10–12] A similar result was proven for certain nonlinear systems,[13] and this fast-switching result has also been extended recently to the stability of the synchronized state of a population of homogeneous nonlinear oscillators in Refs. 3 and 5. This fast-switching result is interesting in the sense that even though the individual static network dynamics do not inherently support synchrony by themselves, the fast-switching system can nevertheless synchronize, as long as the time-averaged static system can be shown to support synchrony.

III. HETEROGENEOUS SWITCHING NETWORKS

A. Our system

Our current effort aims to investigate the behavior of a switching network with heterogeneous elements. To this end, we construct a time-varying network based on our many-population model of phase oscillators, Eq. (1), by using the following connection matrix:

$$\mathbf{K}_{\rho(t)} = \begin{pmatrix} K_{\theta\theta,\rho(t)} & K_{\theta\phi,\rho(t)} \\ K_{\phi\theta,\rho(t)} & K_{\phi\phi,\rho(t)} \end{pmatrix}, \qquad (6)$$

where $\rho(t): \mathbb{R} \to \{A, B\}$ is a binary switching sequence such that

$$\rho(t) = \begin{cases} A, & t \in [m\tau, (m+1)\tau], \quad \text{where } m \text{ is even,} \\ B, & t \in [m\tau, (m+1)\tau], \quad \text{where } m \text{ is odd.} \end{cases} \qquad (7)$$

Thus, the time-dependent connection matrix $\mathbf{K}(t)$ alternates between $\mathbf{K}_A$ and $\mathbf{K}_B$ with a frequency $f = 1/(2\tau)$ Hz. Note that each matrix is "in effect" for equal amounts of time τ (in seconds).

B. Fast and slow switching regimes

The complex order parameter $z_\sigma = r_\sigma e^{i\psi_\sigma}$ introduced in Sec. II A is a measure of the collective coherence of the network and can be interpreted as the centroid of all phase variables within the population. If the switching is sufficiently frequent, z_σ is approximately constant during the dwell time τ for which each static matrix is "in effect," and we have

$$z_\sigma(t) \approx \langle z_\sigma(t) \rangle, \qquad (8)$$

where $\langle z_\sigma(t) \rangle \equiv 1/2\tau \int_t^{t+2\tau} z_\sigma(t') dt'$ is the time-averaged order parameter over one complete switching cycle. While this condition holds for sufficiently fast switching, Eq. (8) is not

sufficient to define the fast-switching regime. For example, if the coupling strength η and the connection matrices are such that the network remains incoherent, Eq. (8) holds even for slow switching.

To better distinguish the two regimes, we define a characteristic time τ^*. Based on the linearization described in Sec. II A, we expect a perturbed order parameter to approach its asymptotic value exponentially, i.e., $\sim e^{st}$. Thus, we use $\tau^* = 1/\text{Re}(s)$ as a rough estimate of how fast the network can respond to the perturbations that arise from switching. Using this definition, a switching network is in the "slow regime" if the static matrix dwell time τ is larger than the largest characteristic time for the connection matrices $\mathbf{K}_A$ and $\mathbf{K}_B$, i.e., $\tau \gg \max(\tau_A^*, \tau_B^*)$. In other words, under slow switching, the order parameters have sufficient time to change appreciably (if they are not already at their asymptotic values) before the next switching event occurs. For fast switching, $\tau \ll \max(\tau_A^*, \tau_B^*)$; in this case, the order parameters do not have time to change appreciably before the next switching event takes place.

By taking the time average of the dynamical equations for the order parameters in Eq. (5) over one complete switching cycle, and assuming fast switching conditions so that Eq. (8) holds, we have

$$\frac{dz_\sigma}{dt} = (i\Omega_\sigma - \Delta_\sigma) z_\sigma + \frac{\eta}{2} \sum_{\sigma' = \theta, \phi} \langle K_{\sigma,\sigma'} \rangle [z_{\sigma'} - z_{\sigma'}^* z_\sigma^2], \qquad (9)$$

where $\sigma = \theta, \phi$. Thus, for sufficiently fast switching, it is clear that the macroscopic behavior of the switching network described by Eqs. (1), (6), and (7) is explicitly controlled by the "static" average connection matrix,

$$\langle \mathbf{K} \rangle = \begin{pmatrix} \langle K_{\theta\theta,\rho(t)} \rangle & \langle K_{\theta\phi,\rho(t)} \rangle \\ \langle K_{\phi\theta,\rho(t)} \rangle & \langle K_{\phi\phi,\rho(t)} \rangle \end{pmatrix} = (\mathbf{K}_A + \mathbf{K}_B)/2.$$

In the following, we examine how the switching system transitions to this fast-switching behavior in several nonintuitive cases.

C. Transition from incoherence to coherence under fast switching

In our first example, we consider the situation in which neither $\mathbf{K}_A$ nor $\mathbf{K}_B$ support synchrony under static (non-switching) conditions, while the average matrix $\langle \mathbf{K} \rangle$ does (under static conditions). In this case, the occurrence of synchronization in the "fast-switching" system is perhaps surprising: it may seem counterintuitive that switching between matrices that do not separately support synchronization under static conditions can nevertheless lead to synchronization if the switching frequency is fast enough. In fact, we do observe this behavior, and we describe the mechanism that gives rise to it below.

Under slow switching, the switching system remains in the incoherent state ($r_\sigma = 0$). We wish to show that the characteristic time τ^* calculated from the linearized incoherent state gives an accurate prediction for the critical frequency for the fast switching regime. From the discussion in Sec.

II A, the linear stability s of the incoherent state for a (static) matrix $\mathbf{K}$ can be directly calculated by setting the determinant of the matrix in Eq. (3) to zero, i.e.,

$$\det\left[\eta\mathbf{K} - \begin{pmatrix} 1/g_\theta(s) & 0 \\ 0 & 1/g_\phi(s) \end{pmatrix}\right] = 0. \quad (10)$$

Using Cauchy–Lorentz distributions for $G_\sigma(\omega_\sigma)$, one can explicitly calculate the contour integral in the complex function $g_\sigma(s)$,

$$g_\sigma(s) = \frac{1}{2}\int_{-\infty}^{\infty} \frac{G_\sigma(\omega_\sigma)}{s - i\omega_\sigma}d\omega_\sigma = \frac{1}{2(s + \Delta_\sigma) - i\Omega_\sigma}.$$

Substituting $g_\sigma(s)$ back into Eq. (10) and setting $\Delta_\theta = \Delta_\phi = \Delta$ and $\Omega_\theta = \Omega_\phi = \Omega$, one can solve the resultant complex quadratic equation for s. The solution,

$$s(\mathbf{K}, \eta) = \tfrac{1}{4}(-4\Delta - \eta Tr(\mathbf{K}) \pm \eta\sqrt{Tr^2(\mathbf{K}) - 4\,det(\mathbf{K})} + 2i\Omega), \quad (11)$$

gives the linear stability of the incoherent state of the network with a given static connection matrix $\mathbf{K}$ and coupling strength η.

To develop a concrete example, recall from Sec. II A that for static traceless connection matrices and $G_\theta = G_\phi$, synchronization is possible for an appropriately selected value of η as long as the determinant of the connection matrix is negative. If the determinant is positive, synchronization is not possible for any η. Accordingly, we choose the traceless matrices

$$\mathbf{K}_A = \begin{pmatrix} c & -a \\ a & -c \end{pmatrix} \quad \mathbf{K}_B = \begin{pmatrix} c & a \\ -a & -c \end{pmatrix}, \quad (12)$$

where a and c are real numbers. Then, if $a^2 \geq c^2$, we have $\det(\mathbf{K}_A) \geq 0$ and $\det(\mathbf{K}_B) \geq 0$, and neither matrix supports synchrony under static conditions for any value of η.

In the example below, we use $a = 2$, $c = 1$, $\Delta = 1$, and $\Omega = 0$. Substituting these values into Eq. (11) gives

$$s(\mathbf{K}_A) = s(\mathbf{K}_B) = -\Delta \pm i\frac{\sqrt{3}}{2}\eta.$$

Therefore, for any choice of η, the incoherent states ($r_\theta = r_\phi = 0$) for this set of connectivity matrices are exponentially stable with a characteristic decay time inversely proportional to Δ, the width parameter of the frequency distribution of the phase oscillators. That is,

$$\tau^* = 1/|\text{Re}(s)| = 1/\Delta. \quad (13)$$

Based on the arguments above, we expect that for switching frequencies larger than $1/\tau^* = \Delta$, the time evolution of the switching network should be close to that of a static network with connectivity matrix $\langle\mathbf{K}\rangle = \begin{pmatrix} c & 0 \\ 0 & -c \end{pmatrix}$. Note that in this particular case, $\langle\mathbf{K}\rangle$ is diagonal, so that the corresponding static network consists of two independent simple Kuramoto systems with coupling $c\eta$ and $-c\eta$. For $\eta \geq \eta^* = 2/c$, the θ population will synchronize, and the ϕ population will not. We now examine the behavior of the switching system as this fast-switching limit is approached.

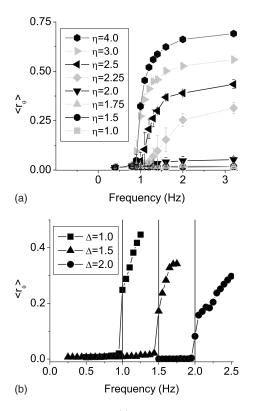Figure 1(a) shows the time-averaged asymptotic order

FIG. 1. Incoherence to coherence: (a) The time-averaged order parameters $\langle r_\theta \rangle$ vs the switching frequency f for the θ population with $\Delta = 1$ and a range of η values (see legend). (b) The dependence of the critical transition for three different sets of parameters: ($\Delta = 1$, $\eta = 4$; $\Delta = 1.5$, $\eta = 5$; and $\Delta = 2$, $\eta = 5.5$).

parameter $\langle r_\theta \rangle$ for the synchronizing population (θ) as the switching frequency is varied. (For all our numerical examples, our population size is 10 000 or more to minimize fluctuations.) The curves represent various values of the overall coupling strength η as listed in the figure legend. For weak coupling ($\eta < \eta^* = 2$), the time-averaged order parameters remain small for all values of the switching frequency. Then, for sufficiently strong coupling ($\eta > \eta^* = 2$), the θ population transitions from incoherence to coherence at the predicted critical frequency $f^* = 1/\tau^* = \Delta = 1$ Hz, and the expected fast-switching behavior is immediately apparent. Note that the transition occurs at the same critical frequency for all the curves in Fig. 1(a), in accordance with the prediction that $f^* = \Delta$ is independent of η. To test the dependence on Δ, we repeated the experiment for various values of Δ. The time-averaged asymptotic order parameter $\langle r_\theta \rangle$ for the θ population is plotted as a function of frequency in Fig. 1(b) for various values of Δ and $\eta > \eta^*$. As predicted, the population transitions from incoherence to coherence at the critical frequencies given by $f^* = \Delta$.

In Figure 2(a), we examine the behavior of the other population (ϕ) as the switching frequency is varied. Again, the curves correspond to various coupling strengths, and it can be seen that for $\eta > \eta^* = 2$, the time-averaged asymptotic order parameter $\langle r_\phi \rangle$ rises, reflecting a modest amount of synchrony in this population, and then gradually falls with increasing switching frequency. The latter behavior is expected, since $\langle\mathbf{K}\rangle$ is diagonal, and the ϕ population should be
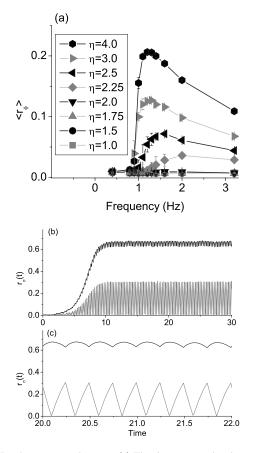
FIG. 2. Incoherence to coherence: (a) The time-averaged order parameters $\langle r_\phi \rangle$ vs the switching frequency f for the ϕ population with a range of η values (see legend). (b) The time course of the instantaneous order parameters $r_\sigma(t)$ in the fast switching regime ($f=2$ Hz, $\eta=4$, $r_\theta(t)$—upper black curve, $r_\phi(t)$—lower gray curve). (c) A magnification of (b) on an expanded time scale. Note the large oscillations in the frustrated order parameter $r_\phi(t)$—lower (gray) curve.

incoherent in the fast-switching limit. However, the occurrence of synchrony for intermediate switching frequencies near $f^*=1/\Delta$ is perhaps surprising. This can be understood by considering graphs of the order parameter magnitudes versus time as shown in Figs. 2(b) and 2(c) for $\eta=4$. Panel (c) shows a segment of the data in panel (b) on an expanded time scale. It can be seen that the order parameter for the θ population (black curve) approaches a high value and fluctuates about it with small amplitude; note that this behavior is consistent with Eq. (8). The order parameter for the ϕ population (gray curve), however, undergoes very large fluctuations that extend down to zero, and therefore does not satisfy Eq. (8).

These excursions through zero are due to the effects of the off-diagonal elements of $\mathbf{K}_A$ and $\mathbf{K}_B$. Because the dwell time τ is not small, a non-negligible synchronizing signal from the θ population is fed into the ϕ population, counteracting the negative desynchronizing signal that is present due to the intrapopulation coupling. These dynamics can be conveniently described in terms of the order parameter phasors. An examination of these phasors (not shown) reveals that whereas the θ phasor retains a large magnitude, the ϕ phasor makes excursions back and forth through zero: at every

switch, it shrinks to zero and then grows again, alternating between an in-phase (0 radians) and an antiphase (π radians) relationship with the θ phasor.

As the frequency increases, r_θ remains large. Meanwhile, r_ϕ fluctuates about zero, but with progressively less time to grow between switches. As long as the dwell time τ is long enough for the synchronizing signal from the θ population to have an effect, there will be some degree of synchronization in the ϕ population. Therefore, the expected fast-switching limiting behavior of the ϕ population requires a higher switching frequency in order to become evident.

The particular case presented above is special in that the matrices involved are all traceless. This provides a convenient illustrative example that takes advantage of the fact that synchronization in a network with a static traceless matrix hinges on the determinant of the matrix, as described above. We also examined a more generic class of matrices where $\text{Tr}(\mathbf{K}) \neq 0$. Although we do not present those results here, the fast-switching results described above also hold for this more general situation.

D. Transition from coherence to incoherence under fast switching

In this section, we will examine the reverse situation in which both $\mathbf{K}_A$ and $\mathbf{K}_B$ support coherence in the static condition. For this case, we again confirm that the network dynamics in the fast switching regime behave according to the time-averaged connection matrix $\langle \mathbf{K} \rangle$, and the transition to this fast-switching limiting behavior also reveals interesting order parameter phasor dynamics.

For our numerical experiments, we again consider traceless matrices. Specifically, we choose

$$\mathbf{K}_A = \begin{pmatrix} a & -c \\ c & -a \end{pmatrix} \quad \mathbf{K}_B = \begin{pmatrix} -b & -c \\ c & b \end{pmatrix}, \quad (14)$$

where a, b, and c are arbitrary real numbers. Choosing $a=b$ and requiring $a^2 > c^2$ ensures that $\mathbf{K}_A$ and $\mathbf{K}_B$ have negative determinants. Then, referring to Table I, choosing $|\eta| > 2\Delta/\sqrt{a^2-c^2}$ ensures that the corresponding static networks synchronize. Meanwhile, the average matrix

$$\langle \mathbf{K} \rangle = \begin{pmatrix} 0 & -c \\ c & 0 \end{pmatrix}$$

is also traceless, but has a positive determinant for all $c^2 > 0$. Thus, while $\mathbf{K}_A$ and $\mathbf{K}_B$ each support synchrony under static conditions, $\langle \mathbf{K} \rangle$ does not.

In the following, we use $a=b=\sqrt{2}$, $c=1$, and $\eta=4$. As in our previous example, we have set $\Delta=1$ and $\Omega=0$. Solving for the equilibrium states in the static condition using Eq. (5), we obtain the values reported in Table II.

To illustrate the fact that the switching system transitions from coherence to incoherence when the switching frequency is sufficiently fast, we perform the following numerical experiment, illustrated in Fig. 3. First, we integrate our system using connectivity matrix $\mathbf{K}_A$ under static, nonswitching conditions until the order parameters settle at their asymptotic values given in Table II. Then, at $t=0$, we initiate fast switching at $f=2.6$ Hz. The graph shows that the order

TABLE II. Coherence to incoherence transition: List of equilibrium states and their stabilities.

$\mathbf{K}_A$	$r_\theta = 0.670\,75$
	$r_\phi = 0.338\,92$
	$|\psi_\phi - \psi_\theta| = 0$
	$s = -2.4215 \pm 0.384\,28i$
$\mathbf{K}_B$	$r_\theta = 0.338\,92$
	$r_\phi = 0.670\,75$
	$|\psi_\phi - \psi_\theta| = \pi$
	$s = -2.4215 \pm 0.384\,28i$
$\langle \mathbf{K} \rangle$	$r_\theta = r_\phi = 0$
	$s = -\Delta \pm \eta/2i$

parameters undergo a few oscillations and quickly decay to zero, confirming that the incoherent state is indeed attracting in the switching network. We include in Fig. 3 the behavior exhibited by a nonswitching network with connectivity matrix $\langle \mathbf{K} \rangle$ initiated in the same way (dotted curves). It can be seen that the oscillations follow the dotted curves rather well, indicating that the transient behavior of the switching system is consistent with that of the average nonswitching system. One should also note that the characteristic time for the convergence of the network toward the incoherent state is consistent with the calculated linear stability of the incoherent state (see Table II) for the static average matrix $\langle \mathbf{K} \rangle$, i.e., $\tau^* \approx |1/\mathrm{Re}(s)| = 1/\Delta = 1$ s.

Next, we calculate the time-averaged order parameters once transients have passed, and plot the results versus frequency. This is shown in Fig. 4. One can see that as the switching frequency increases, the degree of coherence within the populations gradually decreases and vanishes for switching frequencies larger than a critical value f^* at approximately 1.1 Hz.

We note that the linear stability theory used in the previous section led to a good prediction of the critical frequency because the order parameters remained close to their asymptotic values (i.e., the incoherent state with $r_\sigma = 0$) at each switch. However, this is no longer true in the present case: immediately after a switch, the order parameters are far from the asymptotic values that correspond to the currently
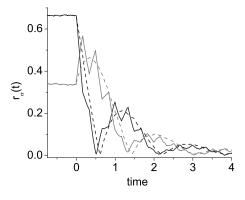
FIG. 3. Coherence to incoherence transition: Transient behavior of the order parameters $r_\sigma(t)$ in time. The connectivity matrix $\mathbf{K}_A$ is in effect for $t < 0$. For $t \geq 0$, fast switching takes place ($f = 2.6$ Hz). The dotted lines represent the order parameters of the corresponding static average network initialized in the same manner. Black curves, r_θ; gray curves, r_ϕ.
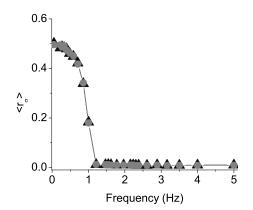
FIG. 4. Coherence to incoherence transition: The time-averaged order parameters $\langle r_\sigma \rangle$ vs switching frequency f. No appreciable synchronization is observed for $f \gtrsim 1.1$ Hz. Black triangles, r_θ; gray circles, r_ϕ.
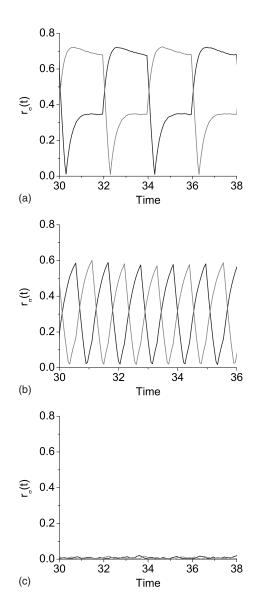
FIG. 5. Coherence to incoherence transition: The order parameters $r_\sigma(t)$ vs time for switching frequencies (a) $f = 0.25$ Hz, (b) $f = 0.90$ Hz, and (c) $f = 1.80$ Hz.
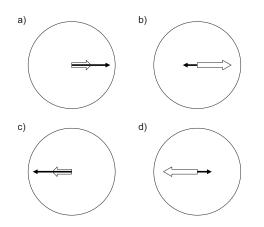
FIG. 6. Incoherence to coherence transition: Asymptotic order parameter phasors corresponding to two complete switching cycles (total time 4τ) in Fig. 5(a).

active connectivity matrix. This can be seen in Figs. 5(a)–5(c), in which we plot the instantaneous order parameters versus time for three different switching frequencies. For the slow switching in (a), each order parameter alternates between approaching a highly synchronized asymptotic state (high $r \approx 0.670\,75$) and a less synchronized asymptotic state (low $r \approx 0.338\,92$) as given in Table II. An important feature is that when a population is in its more synchronized asymptotic state, the next switch causes the order parameter to decay immediately down to zero, indicating that the population becomes completely desynchronized. The population then reorganizes itself and the order parameter increases again as the population approaches its less synchronized asymptotic state. Due to this process, the order parameters fluctuate significantly within the duration of one complete switching cycle, and the "fast switching" condition of Eq. (8) is not satisfied.

As the switching frequency is increased, the transients are shortened. In Fig. 5(b), the order parameters are not able to reach their asymptotic equilibrium states before the next switch takes place. However, transient desynchronization between switches still occurs, as the order parameter excursions to zero described above are still evident. In Fig. 5(c), the higher switching frequency has essentially eliminated all transients, and because the excursions to zero persist, the order parameters hover close to zero.

This behavior, especially the excursions to zero, can be understood by examining the phases ψ_σ of the complex order parameters $r_\sigma e^{i\psi_\sigma}$ [see Eq. (2)]. Recall that in the original Kuramoto system, there is only one population of oscillators. Consequently, the order-parameter phase ψ is not important, since one can always move to a corotating frame in which ψ is zero. This is equivalent to choosing the natural frequency distribution $G(\omega)$ such that it is centered at zero. But because our system has two interacting populations of oscillators, the two order parameter phases can have a nontrivial relationship.

Figure 6 shows a sequence of diagrams illustrating the asymptotic states of the complex order parameters corresponding to Fig. 5(a). These order parameters are drawn as phasors on a unit circle where the lengths and angular orientations of the phasors are given by r_σ and ψ_σ, respectively. When $\mathbf{K}_A$ is in effect [(a) and (c)], the phasors settle into an in-phase state ($\psi_\theta - \psi_\phi = 0$), and when $\mathbf{K}_B$ is in effect [(b) and (d)], the phasors settle into an antiphase state ($|\psi_\theta - \psi_\phi| = \pi$). Thus, for sufficiently low-frequency switching, the switching system cycles among these four states. We draw attention to the evolution of the phasors. When a switch occurs, the shorter phasor grows—see the white phasor in transitions (a)$\rightarrow$(b) and (c)$\rightarrow$(d), and the black phasor in transitions (b)$\rightarrow$(c) and (d)$\rightarrow$(a). Meanwhile, the longer order-parameter phasor shrinks to zero, reflecting the active desynchronization of this population, and then reemerges "on the other side," with a different phase relative to the other phasor. This is observed in the black phasor for transitions (a)$\rightarrow$(b) and (c)$\rightarrow$(d), and in the white phasor for transitions (b)$\rightarrow$(c) and (d)$\rightarrow$(a). Thus, taking note of the order-parameter phases as in Fig. 6 reveals that a complete cycle of the switching system actually consists of *four* states and has a duration of 4τ. [If one only considered the order-parameter magnitudes as in Fig. 5(a), one might erroneously conclude that a complete cycle consists of two states and is completed in time 2τ.]

On the other hand, notice that if one observes the asymptotic order-parameter phasor arrangement at every other switch, i.e., at frequency $1/2\tau$—for example, imagine switching between the states in Figs. 6(a) and 6(c)—then both phasors are seen to make complete excursions through zero. Thus, if the switching frequency is slow enough, the phasors reorient their phases by π radians every two switches. As the switching frequency increases, this process continues, but there is progressively less time for the order parameters to grow between switches. Thus, the populations synchronize less and less for increasing switching frequency.

E. Resonance desynchronization

Lastly, we want to demonstrate that the order-parameter interaction described in the two cases mentioned above can create an interesting resonance phenomenon. To illustrate, we choose our matrices so that the static $\langle \mathbf{K} \rangle$ can support coherence, and we again choose $\mathbf{K}_A$ and $\mathbf{K}_B$ as in Eq. (14). But for this case, we want the determinant of the average matrix

$$\langle \mathbf{K} \rangle = \begin{pmatrix} \dfrac{a-b}{2} & -c \\ c & -\dfrac{a-b}{2} \end{pmatrix}$$

to be negative. Thus, we choose a, b, and c such that $(a-b)^2/4 > c^2$.

Figure 7 shows the asymptotic time-averaged order parameters versus switching frequency for $a=5$, $b=2$, $c=1$, and $\eta=4$. As expected, the network synchronizes for both slow and fast switching frequencies. However, as the frequency sweeps through intermediate switching frequencies, the order parameter decays to small values, remains small over an interval (approximately 1.5–2.25 Hz), and then increases again.
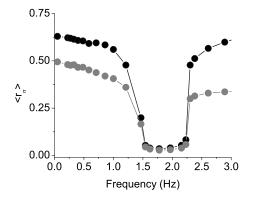
FIG. 7. Coherence to coherence transition: The time-averaged order parameters $\langle r_\sigma \rangle$ vs switching frequency f for switching between connectivity matrices $\mathbf{K}_A$ and $\mathbf{K}_A$ (see text). Black, r_θ; gray, r_ϕ.

This behavior corresponds to a resonance phenomenon in which the switching time scale approximately matches the phasor reorientation time scale as the phasors cycle among the states depicted in Fig. 6. In terms of the oscillators, if the switching time scale is approximately equal to the time scale of active synchronization and desynchronization in the two oscillator populations, then the system is in a "frustrated" state and cannot appreciably synchronize. This novel desynchronization mechanism, therefore, arises from the conflicting tendencies of the two oscillator populations as the connectivity switches back and forth, and an accurate description of this mechanism requires not just the order-parameter magnitudes r_σ, but also the order-parameter phases ψ_σ. We call this effect "resonance desynchronization."

For fast switching, synchronization is seen to return in Fig. 7 for $f \gtrsim 2.25$ Hz. Here, the resonance condition is violated, and the switching occurs so quickly that the order-parameter phasors are unable to complete their excursions toward zero before the next switch occurs. Thus, the π-radian phase reorientation described above does not occur. Instead, the order parameters display a "ratcheting" behavior that gives rise to the expected synchronization in the fast-switching limit.

IV. CONCLUSION

In this work we show that switching networks, under sufficiently fast switching, exhibit behavior characteristic of a static network with the corresponding average connectivity, extending previous results found in the literature to the case of networks that consist of two large populations of heterogeneous oscillators. Furthermore, by examining the dynamics of switching networks as this fast-switching limit is approached in several nonintuitive cases, we identify novel synchronization and desynchronization mechanisms that arise in such systems, and point out the important dynamics exhibited by the order-parameter phasors in systems involving more than one distinct population of oscillators.

We believe that these mechanisms have much wider relevance. Many networks of interest naturally consist of multiple interacting subpopulations. For example, dynamics in neuronal networks typically involve many functional layers and a diverse set of interacting elements (e.g., excitatory pyramidal neurons, inhibitory interneurons, and modulating glia). Connectivity among these elements and/or subpopulations is also rarely static in time. In nature and in many engineering applications, interacting networks of networks with time-varying connectivity are also not uncommon. Furthermore, it has recently been pointed out in the literature that systems without obviously distinguishable subpopulations can nevertheless dynamically segregate themselves into distinct interacting clusters or communities.[14] Although the time-varying multipopulation Kuramoto system used here is somewhat idealized, it does provide an analytically solvable model in which the fundamental mechanisms of multipopulation dynamics can be explored. With recent results on the generalization of the Kuramoto model to other nontrivial topologies[15,16] and with chaotic units,[17–19] this result also suggests a starting point for the investigation of time-varying multipopulation interactions in an even more general setting.

[1] See, for example, S. H. Strogatz, Nature **410**, 268 (2001); R. Milo *et al.*, Science **298**, 824 (2002); M. Girvan and M. E. J. Newman, Proc. Natl. Acad. Sci. U.S.A. **99**, 7821 (2002); R. Milo *et al.*, Science **303**, 1538 (2004); M. E. J. Newman and M. Girvan, Phys. Rev. E **69**, 026113 (2004); M. Kurant and P. Thiran, Phys. Rev. Lett. **96**, 138701 (2006); C. Zhou, L. Zemanová, G. Zamora, C. C. Hilgetag, and J. Kurths, *ibid.* **97**, 238103 (2006); there are many others.

[2] T. Stojanovsky, L. Kocarev, U. Parlitz, and R. Harris, Phys. Rev. E **55**, 4035 (1997).

[3] J. D. Skufca and E. M. Bollt, Math. Biosci. **1**, 347 (2004); D. J. Stilwell, E. M. Bollt, and D. G. Roberson, SIAM J. Appl. Dyn. Syst. **5**, 140 (2006).

[4] R. E. Amritkar and C.-H. Hu, Chaos **16**, 015117 (2006).

[5] I. V. Belykh, V. N. Belykh, and M. Hasler, Physica D **195**, 188 (2004).

[6] Y. Kuramoto, in *International Symposium on Mathematical Problems in Theoretical Physics*, edited by H. Araki, Lecture Notes in Physics Vol. 39 (Springer, Berlin, 1975); *Chemical Oscillators, Waves and Turbulence* (Springer, Berlin, 1984); for a review of work on the Kuramoto model, see S. H. Strogatz, Physica D **143**, 1 (2000).

[7] A. T. Winfree, *The Geometry of Biological Time* (Springer, New York, 1980); S. H. Strogatz, Physica D **143**, 1 (2000); J. A. Acebrón, L. L. Bonilla, and R. Spigler, Rev. Mod. Phys. **77**, 137 (2005); K. Wiesenfeld and J. W. Swift, Phys. Rev. E **51**, 1020 (1995); I. Z. Kiss, Y. Zhai, and J. L. Hudson, Science **296**, 1676 (2005).

[8] E. Barreto, B. Hunt, E. Ott, and P. So, Phys. Rev. E **77**, 036107 (2008).

[9] D. Liberzon and A. S. Morse, IEEE Control Syst. **19:5**, 55 (1999).

[10] R. L. Kosut, B. D. O. Anderson, and I. M. Y. Mareels, IEEE Trans. Autom. Control **32:1**, 26 (1987).

[11] R. Bellman, J. Bentsman, and S. M. Meerkov, IEEE Trans. Autom. Control **30:3**, 289 (1985).

[12] J. Tokarzewski, Int. J. Syst. Sci. **18:4**, 697 (1987).

[13] D. Aeyels and J. Peuteman, IEEE Trans. Autom. Control **43:7**, 968 (1998); Automatica **35**, 1091 (1999).

[14] A. Arenas, A. Díaz-Guilera, and C. J. Pérez-Vicente, Phys. Rev. Lett. **96**, 114102 (2006); Physica D **224**, 27 (2006).

[15] D. M. Abrams and S. H. Strogatz, Int. J. Bifurcation Chaos Appl. Sci. Eng. **16**, 21 (2006).

[16] J. G. Restrepo, E. Ott, and J. G. Restrepo, Chaos **16**, 015107 (2006).

[17] A. S. Pikovsky, M. G. Rosenblum, and J. Kurths, Europhys. Lett. **34**, 165 (1996).

[18] H. Sakaguchi, Phys. Rev. E **61**, 7212 (2000).

[19] E. Ott, P. So, E. Barreto, and T. Antonsen, Physica D **173**, 29 (2002).

[20] E. Ott and T. Antonsen, Chaos **18**, 037113 (2008).